Mon. Not. R. Astron. Soc. **266,** 669–677 (1994)

# A non-thermal radio/optical/X-ray source in PKS 2316 − 423

C. S. Crawford and A. C. Fabian
*Institute of Astronomy, Madingley Road, Cambridge CB3 0HA*

Accepted 1993 August 16. Received 1993 August 16; in original form 1993 May 14

**ABSTRACT**

We report observations of PKS 2316 − 423 in the ultraviolet and with the *ROSAT* HRI, where it appears as a bright point source. Optical spectroscopy reveals weak emission lines and a strong, excess blue continuum that is centrally concentrated. The combined optical–ultraviolet continuum spectrum cannot be fitted by any simple combination of a main-sequence stellar spectrum and a late-type elliptical galaxy spectrum, even allowing for intrinsic reddening. A non-thermal, power-law spectrum reddened by less than 0.5 mag fits the optical–ultraviolet spectrum very well, and extrapolates to match both the radio and X-ray fluxes. We suggest that this continuum emission is probably due to a non-thermal source, such as an active nucleus with an optical synchrotron jet. A second weak X-ray source 10 arcsec south of the nucleus may be related to the central source. PKS 2316 − 423 is probably a BL Lac object, orientated at an intermediate angle to our line of sight.

**Key words:** BL Lacertae objects: general – galaxies: individual: PKS 2316 − 423 – galaxies: jets – radio continuum: galaxies – ultraviolet: galaxies – X-rays: galaxies.

## 1 INTRODUCTION

PKS 2316 − 423 is a southern radio source at a redshift $z = 0.0549$, and is associated with the brightest member of the irregular cluster of galaxies Sérsic 159-02 (S1111), which is of Abell richness class 0. The cluster appears to form a wide binary (separated by 6 Mpc) with the cluster Sérsic 159-03 (S1101; $z = 0.056$). PKS 2316 − 423 is a complex 7-arcmin-long, head-tail radio source orientated at a position angle of 50° (Jones & McAdam 1992). VLA imaging barely resolves a double structure in the head and possible twin tails (Ewald 1981; Hjellming & Bignell 1982).

PKS 2316 − 423 was serendipitously detected as a marginally extended (1.5-arcmin) X-ray source (1E231619 − 4223.3) during observations of the Grus Quartet with the *Einstein Observatory* (Maccacaro & Perola 1981). Its 0.2–3.5 keV flux showed possible evidence for variation from $(4.10 \pm 0.34) \times 10^{-12}$ to $(3.3 \pm 0.34) \times 10^{-12}$ erg cm$^{-2}$ s$^{-1}$ over a period of about six months (assuming a power-law spectrum of energy spectral index 0.5 and Galactic hydrogen column density $N_{\rm H} = 3 \times 10^{20}$ cm$^{-2}$). It is included in the *Einstein* Medium-Sensitivity Survey (EMSS; Gioia et al. 1984; Stocke et al. 1991) with a 0.3–3.5 keV flux of $(2.8 \pm 0.1) \times 10^{-12}$ erg cm$^{-2}$ s$^{-1}$ (assuming $N_{\rm H} = 1.9 \times 10^{20}$ cm$^{-2}$ and a power-law spectrum of energy index 0.4; Gioia et al. 1984).

We originally observed the galaxy associated with PKS 2316 − 423 as a part of a sample looking at the optical properties of possible cooling flow galaxies (Crawford & Fabian 1993). Its optical spectrum clearly showed a strong blue excess continuum that appeared anomalous compared to the blue light seen in the central galaxies of cooling flows. We have since pursued this discovery with new ultraviolet and X-ray observations which we report here. Our results are most consistent with the hypothesis that PKS 2316 − 423 contains a strong synchrotron source emitting over the entire radio–X-ray band. From comparison with the few similar objects known, we suggest that the source is in the form of a jet, weakly beaming its emission towards us.

## 2 OBSERVATIONS

### 2.1 Optical data

We observed the elliptical galaxy associated with PKS 2316 − 423 with the AAT in 1987 September, using the IPCS detector on the 25-cm camera of the RGO spectrograph. The seeing was 1.4 arcsec, and the long slit was of width 1.6 arcsec and orientated at a position angle of 90° (near the parallactic angle).

The 2000-s exposure was reduced using the FIGARO package on Starlink. The two-dimensional spectral image was flat-fielded using several summed, dawn-sky exposures, and then wavelength-calibrated using copper-argon arc exposures. The wavelength coverage obtained corresponds to 3265–5115 Å in the rest frame of PKS 2316 − 423. The

image was sky-subtracted using cross-sections well beyond the extent of the galaxy spatial profile and flux-calibrated from observations of three flux standards observed during the night. Atmospheric extinction and Galactic reddening corrections were made, assuming $A_V = 0.053$ and using the prescription of Burstein & Heiles (1978) to scale from the appropriate hydrogen column density of $1.6 \times 10^{20}$ cm$^{-2}$ (Stark et al. 1992), and the extinction law of Seaton (1979). Finally, we applied a slight straightening polynomial to correct for atmospheric dispersion along the slit. The optical spectrum (Fig. 1) shows clear absorption features and weak emission lines at a redshift of 0.0549.

### 2.2 Ultraviolet data

PKS 2316 − 423 was observed in 1990 June with the *International Ultraviolet Explorer* (*IUE*), at low dispersion in both the long-wave (LWP) and short-wave (SWP) primary cameras for 15 420 and 9900 s, respectively (observation numbers SWP38954, LWP18055 and LWP18048). The data were reduced directly from the extended line-by-line images. The instrumental background noise (as obtained from a median-filtered average of cross-sections away from the apertures) was subtracted, and the two-dimensional spectra were flux-calibrated according to the length of exposure using the appropriate calibration tables (Holm et al. 1982; Cassatella & Harris 1983), and corrected for Galactic reddening.

PKS 2316 − 423 is detected in both cameras, but only where the response of *IUE* is most sensitive. The spectrum was extracted from five spatial rows (5.4 arcsec), and the fluxes measured from the most sensitive wavelength ranges (1700–1900 Å, 2750–2910 Å), with a $3\sigma$ upper limit included for the range 1300–1400 Å; these fluxes are shown in Table 1. The errors are determined from the residuals from the rest of the image in this wavelength range, when divided into bins of five spatial pixels (which is beyond the correlation length of the *IUE* errors). No Lyman-$\alpha$ emission was detected at the redshift of PKS 2316 − 423.

**Table 1.** *IUE* fluxes from PKS 2316 − 423.

| Rest Wavelength (Å) | Mean Flux ($10^{-16}$ erg cm$^{-2}$ s$^{-1}$ Å$^{-1}$) |
|---|---|
| 1280 ± 47 | < 8.28 |
| 1707 ± 95 | 5.45 ± 1.03 |
| 2683 ± 76 | 4.02 ± 0.38 |

### 2.3 X-ray data

PKS 2316 − 423 was observed with *ROSAT* in 1992 May–June, using the High Resolution Imager (HRI; further observations are scheduled later in 1993). PKS 2316 − 423 is detected as a strong point source at the centre of the *ROSAT* HRI field. In Fig. 2, we show a contour plot of the whole X-ray image in which several other sources are detected, including the galaxies NGC 7582 and 7590. We obtained a total of 440 ± 21.2 count from the central source in a total exposure of 6153 s. Assuming a hydrogen column density of $1.6 \times 10^{20}$ cm$^{-2}$, this count rate corresponds to a flux of $(6.0 \pm 0.3) \times 10^{-12}$ or $(6.5 \pm 0.3) \times 10^{-12}$ erg cm$^{-2}$ s$^{-1}$ in the observed energy range 0.1–2.4 keV, for assumed power-law spectra of energy indices 0.5 and 1.0, respectively. This is about a factor of 2 higher than the fluxes determined from the *Einstein* observation, which suggests that the source is variable and thus there is a non-thermal origin for the X-ray flux. The inferred intrinsic luminosity of

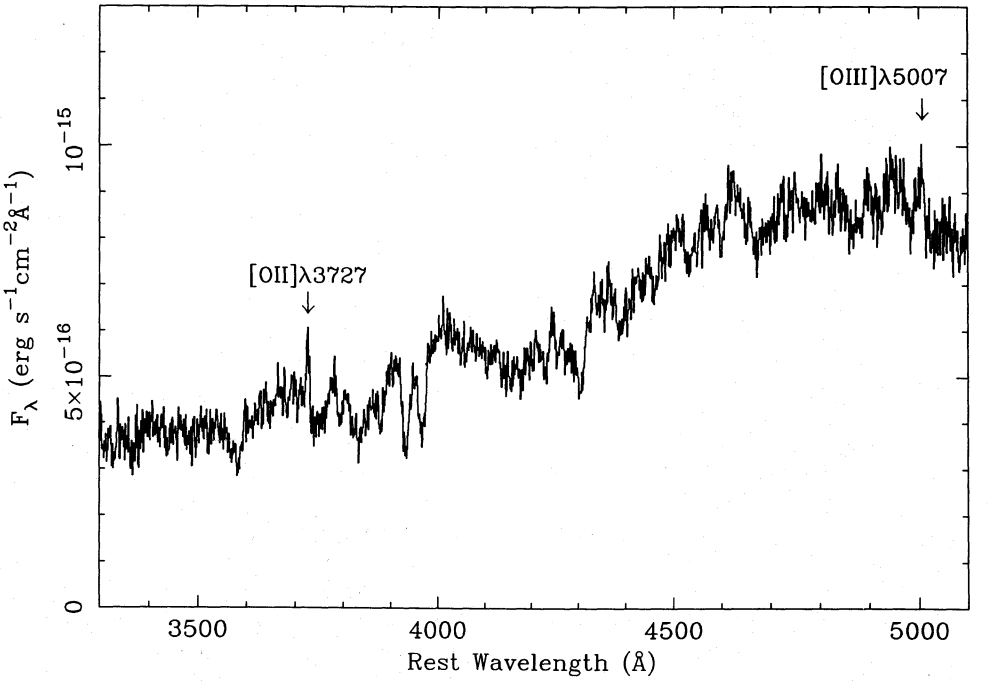


**Figure 1.** The optical spectrum of the central 7 kpc of PKS 2316 − 423.

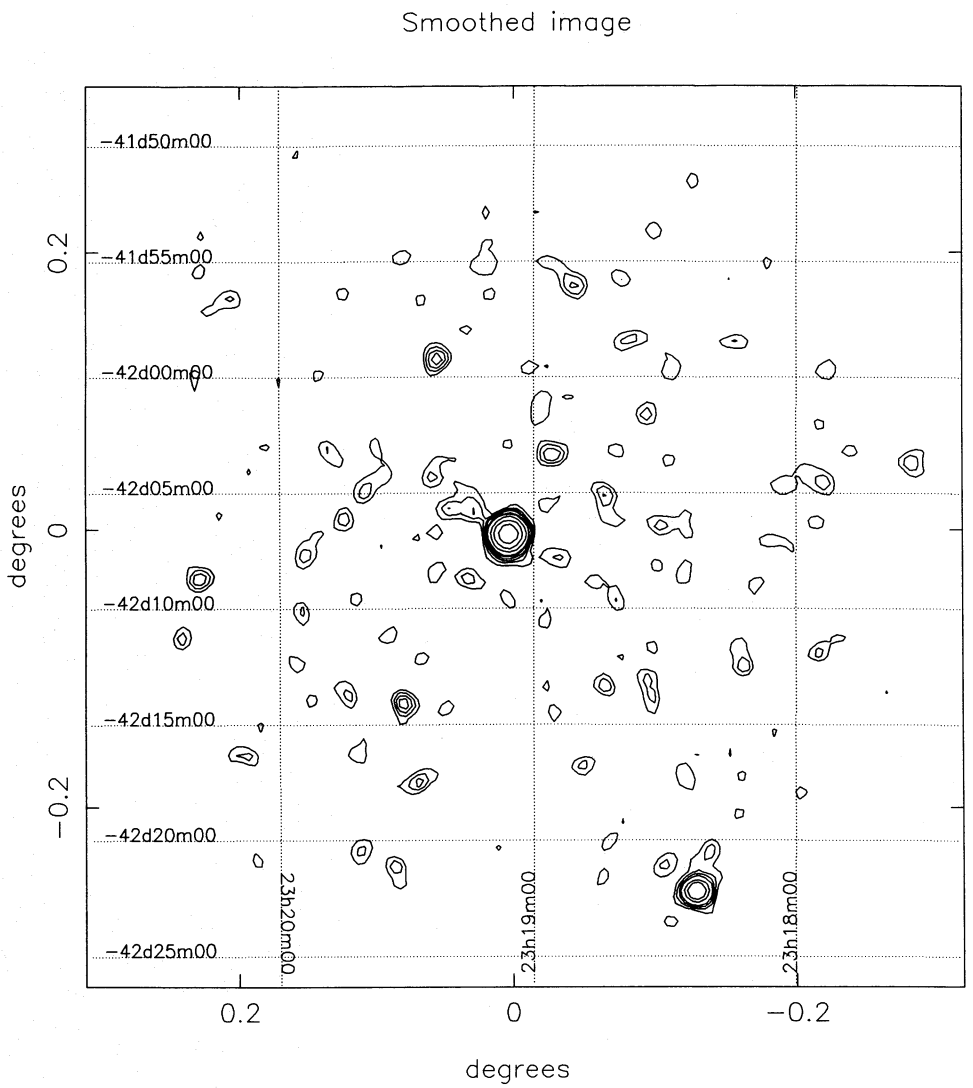


**Figure 2.** The total *ROSAT* HRI field showing all sources detected. The dominant source is associated with PKS 2316 − 423. Coordinates are J2000. Other sources in the field include NGC 7582, a member of the Grus Quartet. The data have been heavily smoothed by a Gaussian FWHM of 45 arcsec, and contours are displayed at 2.7, 3.0, 3.3, 3.6, 4.3, 4.9, 7.4, 12.5, 22.6 and 42.9 count.

$\sim 8.6 \times 10^{43}$ erg s$^{-1}$ is similar to that of other non-quasar AGN (throughout this paper we assume a cosmology of $H_0 = 50$ km s$^{-1}$ Mpc$^{-1}$ and $q_0 = 0$).

A further X-ray source is seen about 10 arcsec (15 kpc) to the south (Fig. 3). This component contains about 4 per cent of the total counts in the source and, if it has the same spectrum as the nucleus, an intrinsic luminosity of $\sim 3.5 \times 10^{42}$ erg s$^{-1}$. It is not orientated on the telescope wobble axis and hence is not an artefact of the dither motion. The surface density of background sources at this flux level is much less than one per square degree, so it is highly unlikely that one should lie within 10 arcsec of PKS 2316 − 423. We conclude that the source to the south is associated with the galaxy.

Azimuthal summing of counts within concentric circles of half-arcsec radial width around the central source shows that it is fitted well by the HRI point spread function, as parametrized in the UK AO-4 Proposer's Guide. Repetition with 15-arcsec-width radial bins shows tentative evidence for an extended component which could contain a count rate as high as that of the point source. If there is a component of very extended X-ray emission – such as might be expected from the surrounding cluster – it has a flat profile, without any indication of a central cooling flow excess.

## 3 ANALYSIS

### 3.1 Spatial optical continuum profile

The 4000-Å break (using the definition given in Bruzual 1983) in the central few kpc ( < 3.5-kpc radius) is very low at 1.4, indicating that there is an extra component of blue optical light over the normal late-type elliptical galaxy population. This is demonstrated further in Fig. 4, where the radial luminosity profile of the *U* band of the optical continuum (rest wavelength 3300–3700 Å) is compared to that of the *B* band of the optical continuum (4650–4850 Å) normalized to the *U* band at radii 10–20 kpc (upper panel). The *U* profile is more peaky than the *B*, indicating a central

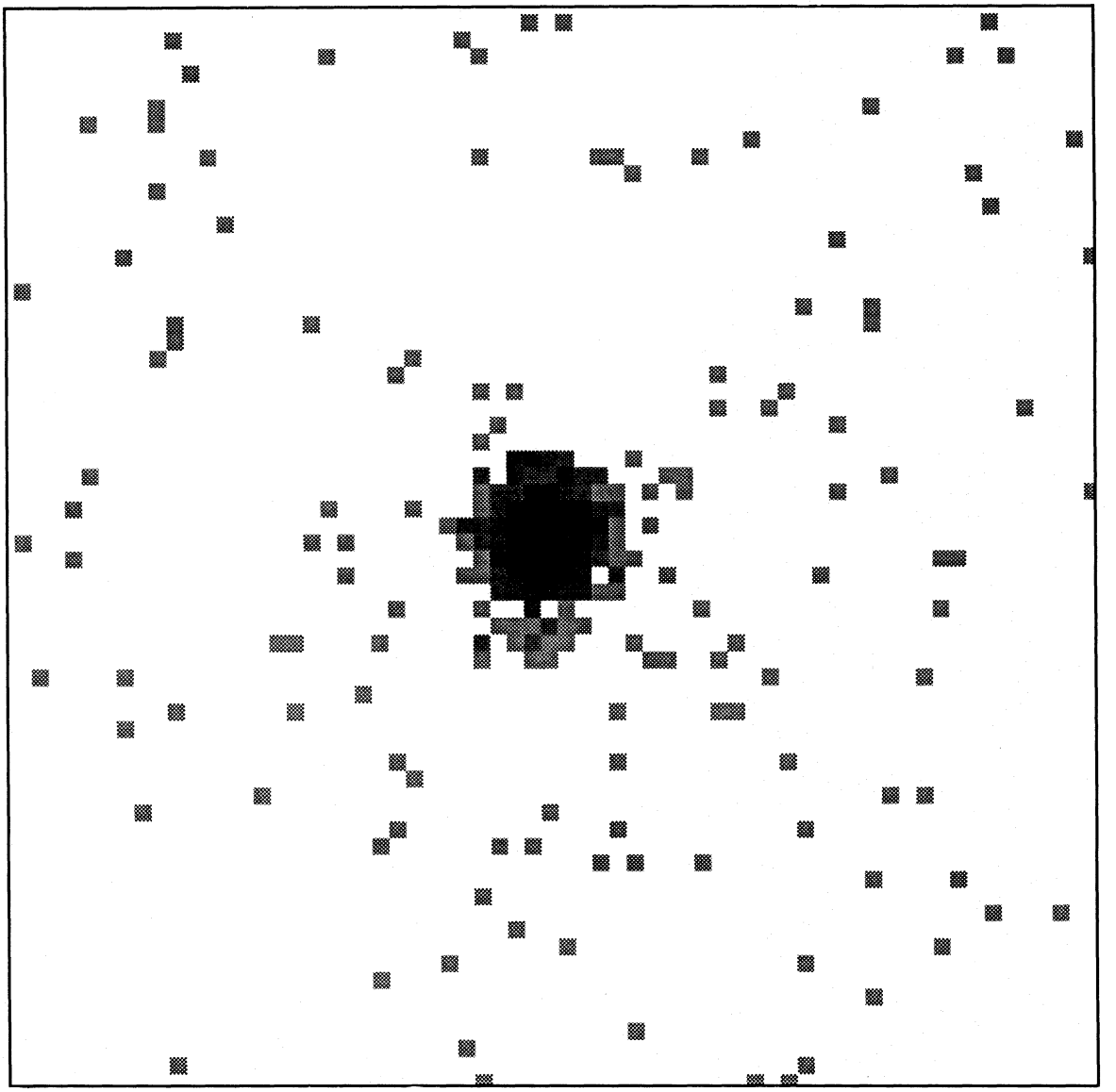

**Figure 3.** Central 2.1 arcmin$^2$ of the HRI field of PKS 2316 − 423, showing the central source and its southern component. North is to the top of the page, east to the left, and the data have been binned into 2-arcsec-square pixels.

ultraviolet excess. The lower panel in Fig. 4 shows the difference between the two profiles, compared to the point spread function from a standard star observed under similar seeing conditions (1.3 arcsec) in the same (observed) region as the *U* continuum. The excess light in PKS 2316 − 423 is compatible with the stellar profile, suggesting that it is not spatially extended along the slit.

The value of the 4000-Å break is slightly higher than the value of 1.33 used by Stocke et al. (1991) to separate the BL Lac object/star-forming galaxy classifications. The low equivalent widths of [O II] $\lambda$3727 (2.61 ± 0.37 Å) and [O III] $\lambda$5007 (1.45 ± 0.24 Å), however, may suggest that the blue light in PKS 2316 − 423 is due to a non-thermal component rather than young star formation. H$\beta$ is not apparent in emission, and the intensity ratio of [O III]/[O II] is ~ 1.3. The emission lines do not appear to form an extended region.

### 3.2 Excess light as young stars

We first investigate whether the extra optical component is emitted by hot young stars, such as are proposed as the origin of the excess blue continuum seen in several central cluster galaxies (Johnstone, Fabian & Nulsen 1987; McNamara & O'Connell 1989; McNamara & O'Connell 1993). We extract an optical spectrum from the central four spatial rows containing the blue excess, corresponding to the light from within a 3.5-kpc radius. In order to combine this with the ultraviolet points, we scale between this reduced optical aperture and the large (10 × 20 arcsec$^2$) oval aperture of *IUE*, which will encompass all the excess blue light. We assume that a young stellar population would follow the optical galaxy distribution, and so fit its spatial profile along the slit in continuum blueward of 3700 Å. We use the

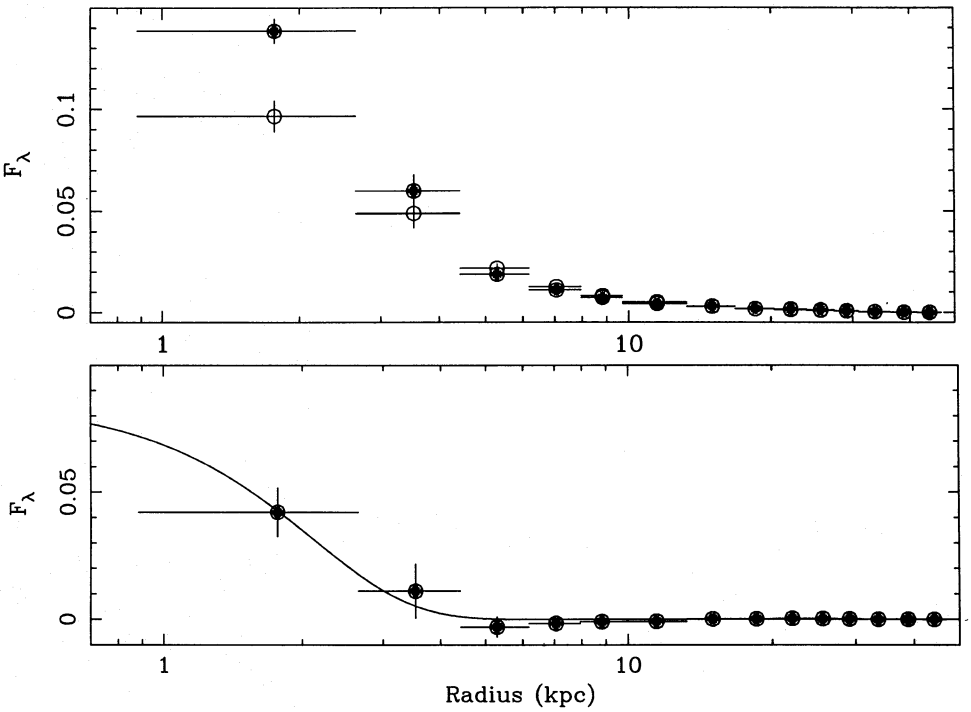


**Figure 4.** Comparative spatial luminosity profiles of the *U* (solid circles) and *B* (open circles) continuum regions, normalized at radii 10–20 kpc (top panel). The lower panel shows the difference of the profiles comparable to a stellar point spread function in the same seeing conditions and (observed) wavelength range. The *y*-axis is in arbitrary units.

best-fitting Lorentzian model to integrate the relative surface brightnesses of the galaxy seen through each aperture and hence form a ratio. For this comparison to be valid, we must assume both that the galaxy profile is circularly symmetric and that each aperture is centred on the galaxy (which it is, according to the pointing information). Under these assumptions we deduce that the optical slit covers only 45 per cent of the total blue light, and hence multiply it to form the combined optical–ultraviolet spectrum shown in Fig. 5.

We fit the optical spectrum with the sum of two components: the spectrum of an elliptical galaxy, and the spectrum of a main-sequence star of spectral type earlier than G0. Single-spectral-type spectra are an adequate representation of any new population, since the light from any IMF is dominated by the most massive stars. The late-type stellar template was taken from a spectrum of the central cluster galaxy associated with the radio source PKS 2354 − 350, which was observed during the same observing run, and which shows a 'normal' elliptical galaxy colour gradient with no optical excess. The spectrum of the main-sequence component was constructed using the Kurucz stellar atmospheres (Kurucz 1979).

Excellent fits to the optical continuum alone can be obtained for the combination of the late-population template with high-mass stars such as type O5 or B0. However, in both cases the ultraviolet light from the young stellar component extrapolates well above the ultraviolet points of PKS 2316 − 423 (Fig. 5). The ultraviolet data are fitted only when the extra component is A0 or later, but spectral types of B5 and later are no longer satisfactory fits to the optical spectrum. The ultraviolet light from a high-mass component would fall below the *IUE* points only if subject to intrinsic reddening of $A_V > 3$ mag, when the template is a much worse fit to the optical spectrum. This remains true even if it is assumed that both apertures cover *all* the blue light from the galaxy.

### 3.3 Excess light as a non-thermal continuum

We show a multifrequency plot for the continuum of PKS 2316 − 423 in Fig. 6, using radio data from the literature and our own *ROSAT*, *IUE* and optical data. We approximate the optical points for the non-thermal component as the level of the blue continuum given by our best-fitting model of a B0 star with an elliptical galaxy, as it accounts for the optical spectrum well (even though it is not a good fit in the ultraviolet). Most of the radio data appear to extrapolate to meet the *ROSAT* HRI detection well, suggesting a common non-thermal origin for the emission. A power-law fit of energy index 0.67 (i.e. $\nu F_\nu \propto \nu^{0.33}$) represents a good fit to the data above $10^9$ Hz, excepting the optical and ultraviolet emission. The only radio point that is incompatible is that observed at 8400 MHz (Wright et al. 1991). We have no obvious explanation for this data point, but note that it may indicate either a variable source, or that the source consists of several components with different spectra.

In seeking to account for the blue light in PKS 2316 − 423 as a non-thermal source, we can relax the optical–ultraviolet scaling constraint that the blue light follows the general galaxy profile. The blue light excess is symmetric about the centre of the galaxy in the optical slit (Fig. 4); both it and the *IUE* and HRI detections are consistent with a point source. As we discuss later, the most obvious non-thermal source operating over such a wide energy range is a jet. The X-ray

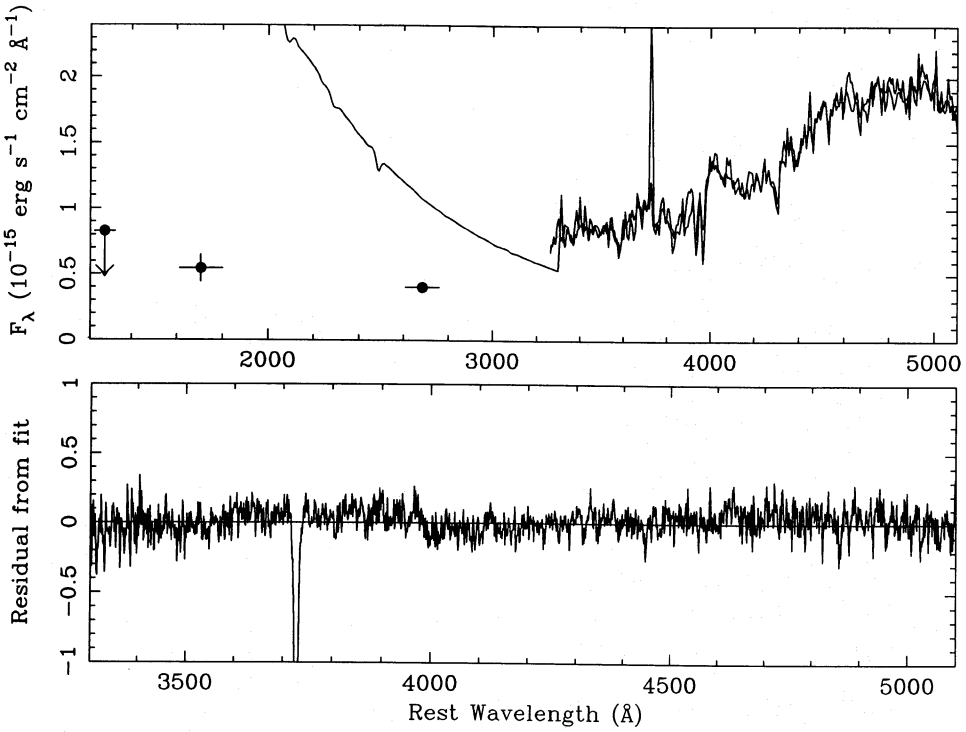


**Figure 5.** Spectral fit to the optical and *IUE* spectrum of PKS 2316 − 423, assuming that the optical slit covers only 45 per cent of the excess blue continuum. The optical spectrum is smoothed by convolving it with a Gaussian of half-width 3 pixel and a total cut-off of 9 pixel. The template shown is B0 stars with the late-type galaxy spectrum of PKS 2354 − 350 without any intrinsic reddening. The top panel shows that a good fit to the optical spectrum extrapolates well above the ultraviolet points, and the bottom panel shows the difference between model and fit in the optical wavelengths. There is an obvious mismatch at [O II] λ3727 because PKS 2354 − 350 has stronger line emission, and the slight deficit around 4000–4200 Å is probably due to differences in metallicity between the template and PKS 2316 − 423.

source 10 arcsec to the south of the nucleus may be due to a knot in such a jet (it is far too luminous to be a binary X-ray source in the host galaxy). If the optical excess continuum also has a second non-thermal component extending beyond 1.2 kpc (e.g. a jet), we would not have detected it, as the optical slit was oriented E–W. The *IUE* aperture could cover both the nucleus and part of any second component extending to the south of the galaxy.

We fit the power law given by the multifrequency data to the optical and ultraviolet spectrum, under two hypotheses: that there is a second component at (i) 10 per cent or (ii) 30 per cent of the nuclear luminosity. We choose these two scalings as representative of the range of possible relative luminosities. We fit the optical spectrum by the sum of a non-thermal component represented by $F_\lambda \propto \lambda^{-1.33}$ (i.e. our $\nu F_\nu \propto \nu^{0.33}$ relation for the radio and X-ray spectrum), and the old-population galaxy template (PKS 2354 − 350) for each of the optical–ultraviolet scalings. The fits still extrapolate to above the *IUE* detections, unless reddening is present. A good fit can be obtained to both the ultraviolet and the optical only if the models are reddened by $A_V$ of 0.5 and 0.2 mag for scalings under hypotheses (i) and (ii) respectively (see Fig. 7). The highest level of reddening still compatible with the depth of the optical absorption line features is $A_V = 0.5$ mag. Thus it appears that any extended optical component cannot be more than 30 per cent of the nuclear luminosity. Without any detection of either Lyman-$\alpha$ or H$\beta$ in emission, we cannot verify whether intrinsic dust is present at such levels, but note that PKS 2316 − 423 is not listed in the *IRAS* catalogue. For both of these models, the blue light component ranges account for ~67 per cent of the flux from PKS 2316 − 423 in the range 3400–3500 Å, and ~25 per cent at 4700–4800 Å.

We have not yet included the possibility that the old stellar population of the galaxy may have its own ultraviolet contribution in the form of an ultraviolet 'rising branch' (e.g. Burstein et al. 1988). The origin of this ultraviolet continuum is not well determined (Ferguson et al. 1991), its level varying widely between elliptical galaxies. We include the light from a putative ultraviolet rising branch of PKS 2354 − 350 at two extremes representing the most and least ultraviolet-active, as determined from mean spectra of optically quiescent elliptical galaxies in Burstein et al. (1988). Whereas in Fig. 5 the template ultraviolet spectrum originated only from the main-sequence stellar component to the fit, in Fig. 7 it is now contributed by both the reddened power law and the galaxy's ultraviolet rising branch (where the galaxy's spectrum has also been reddened). The inclusion of the ultraviolet rising branch makes very little difference to the conclusions, with the ultraviolet spectrum still within the *IUE* data errors (Fig. 7).

When these two extremes of power-law fit are dereddened and the intrinsic luminosities of the excess component at optical and ultraviolet frequencies are plotted on the multi-frequency spectrum (Fig. 6), the 'hidden' luminosity projects very satisfactorily on to the radio–X-ray extrapolation.

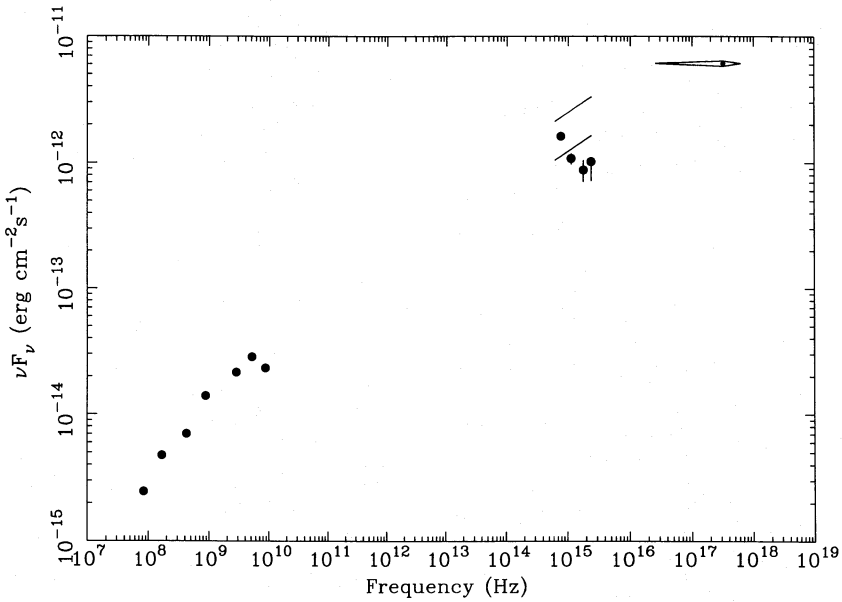


**Figure 6.** Multifrequency plot for PKS 2316 − 423. The X-ray, ultraviolet and optical points are data from this paper. The two straight slopes spanning $5\times10^{14}$ to $3\times10^{15}$ Hz represent the dereddened power-law component fit to the ultraviolet and optical data if the blue light originates in a jet-like component at either 30 per cent (upper slope) or 10 per cent (lower slope) of the nuclear luminosity. Radio data are from the literature: 80 MHz, 160 MHz (Slee 1977); 408 MHz (Robertson & Roach 1990); 843 MHz (Jones & McAdam 1992); 2700 MHz and 5000 MHz (Schimmins 1971; Schimmins & Bolton 1972; Gardner, Whiteoak & Morris 1975); 8400 MHz (Wright et al. 1991).

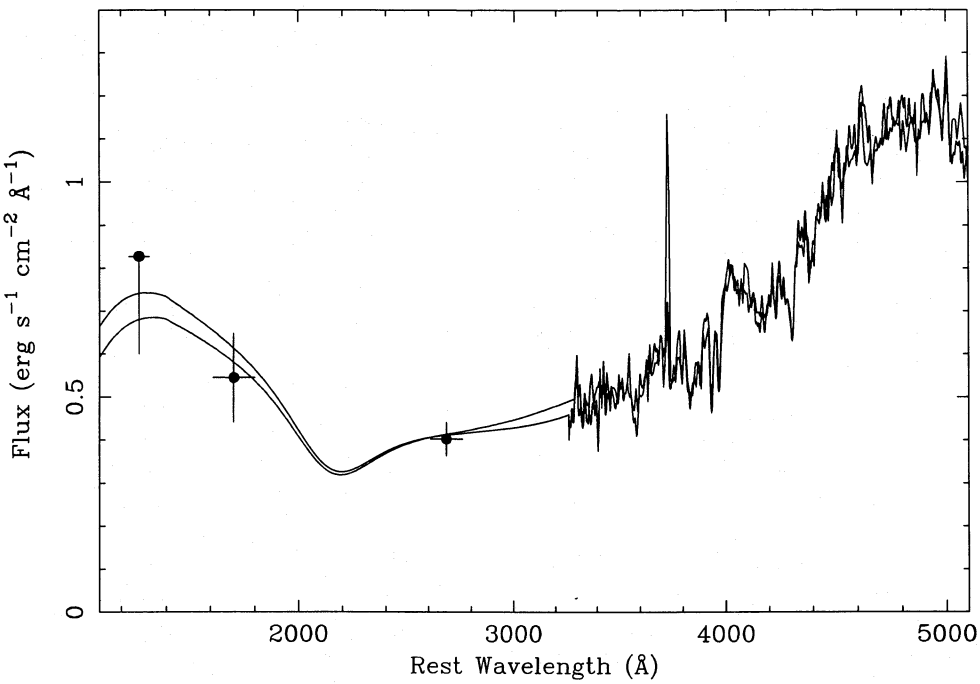


**Figure 7.** The spectral fit of the late stellar template and a power law of slope $\lambda^{-1.33}$ to the optical spectrum, extrapolated to the ultraviolet data. The optical and *IUE* points are scaled in this example assuming that the excess light originates in a nuclear component and a jet-like component at 30 per cent of the nuclear excess luminosity. The power law and galaxy template have been reddened by $A_V$ of 0.5 mag. The two different template spectra over 1100–3300 Å are each obtained assuming extremes of ultraviolet rising branch activity from the old stellar part of the template.

## 4 DISCUSSION

We have found a bright continuum source in PKS 2316 − 423 that radiates over a wide wavelength range. The two-dimensional optical spectra show an unresolved blue central excess, which is detected in the X-rays as a point source (with a second component 10 arcsec distant). There is evidence for variability (but only by a factor of 2) between the *Einstein* and *ROSAT* detections. The combined optical–ultraviolet spectrum cannot be fitted by a stellar spectrum, even allow-

ing for the possibility of intrinsic reddening, but can be accounted for as an elliptical galaxy with the addition of the power-law component, both reddened by $A_V < 0.5$ mag. This result is not substantially changed unless the source has varied by much more than a factor of 2. The excess optical continuum, ultraviolet and X-ray data appear to be a continuation of the radio synchrotron spectrum of PKS 2316−423 (once the effects of intrinsic extinction and reddening have been removed), indicating a common origin for the emission.

Although radio synchrotron emission is common in active galaxies, direct evidence for optical synchrotron radiation is rare, and is found in the form of either jets (M87, 3C 273, 3C 66B, PKS 0521−36, 3C 264: Keel 1988; Macchetto 1992; Crane et al. 1993) or hotspots (3C 20, 3C 33, Pictor A: Keel 1988; Röser 1989). The intrinsic emission from an active nucleus itself may be broad-band and non-thermal, but the dense surrounding gas absorbs and reradiates it so that it does not emerge to the observer as a single power law. Only when the emission is from a jet is it bare enough for little reprocessing to occur. The best examples of X-ray emission associated with a jet are the two nearest radio galaxies, Cen A (Schreier et al. 1979; Feigelson et al. 1981) and Virgo A (Schreier et al. 1982). In both cases the X-ray emission is consistent with an extrapolation of the radio–optical synchrotron spectrum, and in Cen A the X-ray structure correlates with synchrotron knots in the radio jet (Feigelson et al. 1981). The X-ray emission from the jet component is also in each case of comparable brightness to the nuclear emission.

X-ray and optical synchrotron decay times are very much shorter than at radio wavelengths, and both are important for studying sites of the most recent particle acceleration in knots of a radio jet and hence constraining jet emission models. Assuming a single-power-law spectrum for the radio/optical/X-ray spectrum of PKS 2316−423, we find that it is consistent with synchrotron emission from electrons of $\gamma \gtrsim 2 \times 10^7$ in a field with $B \lesssim 10^{-3}$ G. The self-absorption cut-off is then below 100 MHz, and the synchrotron cooling time is less than a year; so variability can be observed in the X-ray flux.

We have estimated from the optical–*IUE* spectrum of PKS 2316−423 that any extended, optical, non-thermal component can at most be 30 per cent of the nuclear luminosity. The distance of 15 kpc to the lower luminosity component in the X-ray image is comparable to the 12-kpc scale seen for the jet in Cen A. Given the proximity of this second X-ray component to the nucleus and its position away from the radio tail(s) (Hjellming & Bignell 1982), we assume that any optical excess continuum is unlikely to originate from a synchrotron hot-spot, and may be just a distant knot in a jet.

PKS 2316−423 forms an interesting comparison to the well-studied BL Lac object/radio galaxy PKS 0521−36 at the same redshift ($z = 0.055$; Danziger et al. 1979; Sparks, Miley & Macchetto 1990). PKS 0521−36 shows a much higher level of non-thermal optical activity, has an extended emission-line region and is highly variable. We speculate that PKS 2316−423 is very similar, except that we are viewing it at a larger angle to the line of sight and hence seeing dilution of the beamed BL Lac activity by the properties of the host galaxy. There is evidence that X-ray selection from samples such as the EMSS finds more 'off-axis' BL Lac objects (Morris et al. 1991). PKS 2316−423 might be such an object whose jet is orientated almost completely out of the line of sight. If this is verified, then it will provide an interesting test case for both the host galaxies of BL Lac objects and their environment.

So far our hypothesis for non-thermal radiation in the optical waveband is supported mainly by the shape of the spectrum. We intend to pursue both high-resolution optical imaging and optical polarization studies to establish unambiguously the non-thermal nature of the excess component in PKS 2316−423. Also, higher resolution radio maps should clearly reveal its structure and enable us to explore more fully the head–tail nature of the extended radio emission. It is possible that the source is better-classified as a wide-angle-tailed source, with the main axis perpendicular to the plane of the sky. This would fit better our BL Lac hypothesis. The secondary X-ray point component suggests that, if the non-thermal source is due to a nuclear jet in this object, then it is directed to the south.

## ACKNOWLEDGMENTS

We thank I. M. Gioia and T. Maccacaro for prompting us to include PKS 2316−423 in our original AAT sample, and M. Bremer for his help with the *IUE* observations. CSC acknowledges the support of a Postdoctoral Fellowship from the Science and Engineering Research Council, and ACF the Royal Society.

## REFERENCES

Bruzual G. A., 1983, ApJ, 273, 105
Burstein D., Heiles C., 1978, ApJ, 225, 40
Burstein D., Bertola F., Buson L. M., Faber S. M., Lauer T. R., 1988, ApJ, 328, 440
Cassatella A., Harris A. W., 1983, in *IUE* ESA Newsletter, 17, 12
Crane P. et al., 1993, ApJ, 402, L37
Crawford C. S., Fabian A. C., 1993, MNRAS, 265, 431
Danziger I. J., Fosbury R. A. E., Goss W. M., Ekers R. D., 1979, MNRAS, 188, 415
Ewald S. P., 1981, PhD thesis, New Mexico Institute of Mining and Technology, New Mexico, USA
Feigelson E. D., Schreier E. J., Delvaille J. P., Giacconi R., Grindlay J. E., Lightman A. P., 1981, ApJ, 251, 31
Ferguson H. C. et al., 1991, ApJ, 382, L69
Gardner F. F., Whiteoak J. B., Morris D., 1975, Aust. J. Phys. Astrophys. Suppl, 35, 1
Gioia I. M., Massacaro T., Schild R. E., Stocke J. T., Liebert J. W., Danziger I. J., Kunth D., Lub J., 1984, ApJ, 283, 495
Hjellming R. M., Bignell R. C., 1982, Sci., 216, 1279
Holm A. V., Bohlin R. C., Cassatella A., Ponz D. P., Schiffer F. H., 1982, A&A, 112, 341
Johnstone R. M., Fabian A. C., Nulsen P. E. N., 1987, MNRAS, 244, 75
Jones P. A., McAdam W. B., 1992, ApJS, 80, 137
Keel W. C., 1988, ApJ, 329, 532
Kurucz K. L., 1979, ApJS, 40, 1
Maccacaro T., Perola G. C., 1981, ApJ, 246, L11
Macchetto F., 1992, in Roland F., Sol H., Pelletier G., eds, Extragalactic Radio Sources – From Beams to Jets. Cambridge Univ. Press, p. 309
McNamara B. R., O'Connell R. W., 1989, AJ, 98, 2018
McNamara B. R., O'Connell R. W., 1993, AJ, 105, 417
Morris S. L., Stocke J. T., Gioia I. M., Schild R. E., Wolter A., Maccacaro T., Della Ceca R., 1991, ApJ, 380, 49
Robertson J. G., Roach G. J., 1990, MNRAS, 247, 387

Röser H.-J., 1989, in Meisenheimer K., Röser H.-J., eds, Hot Spots in Extragalactic Radio Sources. Springer, Berlin, p. 91
Schreier E. J., Feigelson E., Delvaille J., Giacconi R., Grindlay J., Schwartz D., Fabian A. C., 1979, ApJ, 234, L39
Schreier E. J., Gorenstein P., Feigelson E. D., 1982, ApJ, 261, 42
Seaton M. J., 1979, MNRAS, 187, 73P
Shimmins A. J., 1971, Aust. J. Phys. Astrophys. Suppl, 21, 1
Shimmins A. J., Bolton J. G., 1972, Aust. J. Phys. Astrophys. Suppl, 23, 1
Slee O. B., 1977, Aust. J. Phys. Astrophys. Suppl, 43, 1
Sparks W. B., Miley G. K., Macchetto F., 1990, ApJ, 361, L41
Stark A. A., Gammie C. F., Wilson R. W., Bally J., Linke R. A., Heiles C., Hurwitz M., 1992, ApJS, 79, 77
Stocke J. T., Morris S. L., Gioia I. M., Maccacaro T., Schild R. E., Wolter A., Fleming T. A., Henry J. P., 1991, ApJS, 76, 813
Wright A. E., Wark R. M., Troup E., Otrupcek R., Jennings D., Hunt A., Cooke D. J., 1991, MNRAS, 251, 330